# Combined IR and XPS characterization of organic refractory residues obtained by ion irradiation of simple icy mixtures

M. Accolla[1], G. Pellegrino[2], G. A. Baratta[1], G. G. Condorelli[3], G. Fedoseev[1], C. Scirè[1],
M. E. Palumbo[1], and G. Strazzulla[1]

[1] INAF-Osservatorio Astrofisico di Catania, Via Santa Sofia 78, 95123 Catania, Italy
  e-mail: `mario.accolla@oact.inaf.it`
[2] CNR – IMM,Via Santa Sofia 64, 95123 Catania, Italy
[3] Dipartimento di Scienze Chimiche, Università degli Studi di Catania, Viale Andrea Doria 6, 95125 Catania, Italy

## ABSTRACT

*Context.* Multi-year laboratory experiments have demonstrated that frozen icy mixtures containing simple organic and inorganic molecules (such as $H_2O$, $N_2$, $CH_4$, CO, $CO_2$, $C_2H_6$, etc.), if exposed to a flux of energetic ions or UV photons, give rise to new more complex molecules at low temperatures (10–50 K). A fraction of the new synthesized molecules is volatile while the remaining fraction is refractory and therefore it is preserved after the warm-up of the substrate to room temperature. Moreover, a part of the refractory material is formed during the annealing to room temperature, when molecules and radicals into the processed ice become mobile and react to form non-volatile molecules. By means of similar mechanisms, complex organic materials may be formed on the icy surfaces of some objects in the outer solar system, such as trans-Neptunian objects, comets and some satellites of the giant planets: in fact the interaction with solar wind and solar flares ions, solar photons and galactic cosmic rays could produce more refractory materials, analogous to those produced in the laboratory. In some cases, the materials thus synthesized may contain functional groups considered relevant to the pre-biotic chemistry in the hypothesis that interplanetary dust particles, comets and meteoroids contributed to seed the early Earth with the building blocks of life.
*Aims.* The aim of this work is to investigate the chemical similarities and differences between some organic residues left over after ion bombardment (200 keV H⁺) of different ice mixtures followed by subsequent warm up under vacuum to room temperature.
*Methods.* Seven organic residues have been prepared in our laboratory following a procedure involving the proton irradiation of seven different icy mixtures and their warm-up to room temperature. All the organic samples were characterized by FTIR spectroscopy with measurements performed in situ, in the ultra-high vacuum condition preventing any sample degradation. Three of them were selected to be characterized by XPS spectroscopy as well.
*Results.* Among the organic residues presented in this paper, only those containing nitrogen and carbon exhibit the multi-component band centred at $2200\ cm^{-1}$. This multi-component band presents interest from the astrobiological point of view due to its attribution to nitriles (–C≡N) and isonitriles (–N≡C). Our results demonstrate that this band is present in the IR spectra of organic nitrogen residues regardless the use of oxygen-bearing species in the icy mixture. This finding is of interest since the $2200\ cm^{-1}$ band has been observed in some extraterrestrial samples (micro-meteorites) collected in the Antarctica.

**Key words.** astrochemistry – astrobiology – methods: laboratory: solid state

## 1. Introduction

Since the 1970s, several laboratories world-wide investigated the formation of radicals and new species after energetic processing (ion and electron bombardment and/or UV photolysis) of simple organic and inorganic frozen molecules such as $H_2O$, $N_2$, $CH_4$, CO, $CO_2$, $C_2H_6$, etc. (e.g. Greenberg et al. 1972; d'Hendecourt et al. 1986; Moore et al. 2001; Strazzulla et al. 2001; Öberg et al. 2009; Nuevo et al. 2010; Materese et al. 2015; Rothard et al. 2017). It is well known that ion and UV-photon irradiation induce similar chemical alteration on the ices from a qualitative point of view, whereas differences can be observed in the yields of destruction or production of species (see Islam et al. 2014; Muñoz Caro et al. 2014, and references therein). Infrared spectroscopy of frozen samples after the energetic processing shows the appearance of new bands indicating the synthesis of new molecules. Raman spectroscopy of some ion irradiated ices shows the formation of hydrogenated amorphous carbon if the unprocessed icy sample contains simple hydrocarbons

(e.g. Ferini et al. 2004; Palumbo et al. 2004). The organic material synthesized in simple icy mixtures containing H-, C-, N-, and O-bearing molecules is believed to be a good analogue of that expected in some astrophysical objects, such as trans-Neptunian objects (TNOs), cold planetary satellites, comets in the Oort cloud, etc. (e.g. Brunetto et al. 2006; Materese et al. 2014; Urso et al. 2017). The organic material left over after the energetic processing of a simple icy mixture and the following warm-up is commonly called organic residue and remains, at room temperature after the sublimation of the most volatile species, as a yellow-brownish film on the substrate where the icy sample was processed. The literature concerning the study of non-volatiles residues is wide and many references are reported in the following sections. Refractory residues have been usually characterized by infrared spectroscopy that is a non-destructive (but low sensitivity) analytical technique. In recent decades, refractory residues have been studied by high sensitivity analytical methods, such as gas chromatography coupled with mass spectroscopy (GC-MS) and X-ray absorption near-edge

structure (XANES). These techniques allow the detection of complex molecules in the organic residues even if they are present in low abundance. For instance, a multi-diagnostic approach (IR, GC-MS and XANES) has been used to study the organic residues formed after UV photolysis (Materese et al. 2014) and after electron bombardment (Materese et al. 2015) of $N_2$:$CH_4$:CO icy mixtures in relative proportion (100:1:1). In both cases the authors reveal the presence of glycolic acid ($C_2H_4O_3$), 3-hydroxypropionic acid ($C_3H_6O_3$) and urea ($CH_4N_2O$), while lactic acid ($C_3H_6O_3$), oxalic acid ($C_2H_2O_4$), 2-hydroxybutyric acid ($C_4H_8O_3$) and glyceric acid ($C_3H_6O_4$) are detected only in the residue left over after UV irradiation of the sample. Muñoz Caro et al. (2002) and Nuevo et al. (2010) detect some amino acids analysing by GC-MS some refractory residues obtained from photoprocessed astrophysical ice analogue mixtures. Other authors (e.g. Kaiser & Balucani 2001; Hudson et al. 2008; Fedoseev et al. 2015) propose different pathways to form amino acids starting from hydrolysis of nitrogen-rich organic matter formed upon energetic and thermal processing of icy mixtures. The detection of complex molecules in organic residues is considered relevant from the astrobiological point of view in the hypothesis that the delivery of extraterrestrial organic compounds by means of interplanetary dust particles (IDPs), comets and meteorites may have contributed to seed the early Earth with the building blocks of life few billion of years ago (see Cobb et al. 2015; Altwegg et al. 2016, and references therein).

In this paper we study seven different organic residues, each obtained after proton irradiation of seven icy mixtures with different amount of carbon, nitrogen, oxygen and hydrogen bearing species. The seven solid samples are characterized by means of in situ transmittance infrared spectroscopy. Three of these samples are selected to be studied also by X-ray photoelectron spectroscopy (XPS) for more in-depth elemental analysis. These two analytical techniques allow us to stress analogies and differences between the seven samples.

The paper is organized as follows: Sect. 2 describes both the procedure to prepare the seven refractory organic samples and the experimental set-up used to develop and characterize them. In Sect. 3 the experimental results are presented, focusing on the differences and similarities among the IR spectra of the seven samples. Moreover, for three of these samples, an elemental analysis, performed by means of XPS spectroscopy, is displayed and discussed. In Sect. 4 we discuss the experimental results in view of their astrophysical implications in Sect. 5.

## 2. Experimental procedure

### 2.1. Sample preparation and IR spectroscopy

The preparation and the IR characterization of the organic samples are performed in the Laboratory for Experimental Astrophysics (LASp) at INAF – Osservatorio Astrofisico di Catania (Italy). The laboratory is equipped with an experimental setup thought to study the interaction between energetic ions or photons with icy mixtures, analogous to those observed in several astrophysical scenarios. A schematic drawing of the equipment is shown in Fig. 1. The apparatus consists of a stainless steel ultrahigh-vacuum (UHV) chamber, operating at a pressure of around $10^{-9}$ mbar, directly connected to a 200 kV ion implanter (Danfysik 1080-200) able to generate and accelerate an ion beam with energy up to 200 keV per single ionization and finally to aim it at a substrate (acting as sample holder) inside the UHV chamber. The substrate (usually an infrared-transparent window
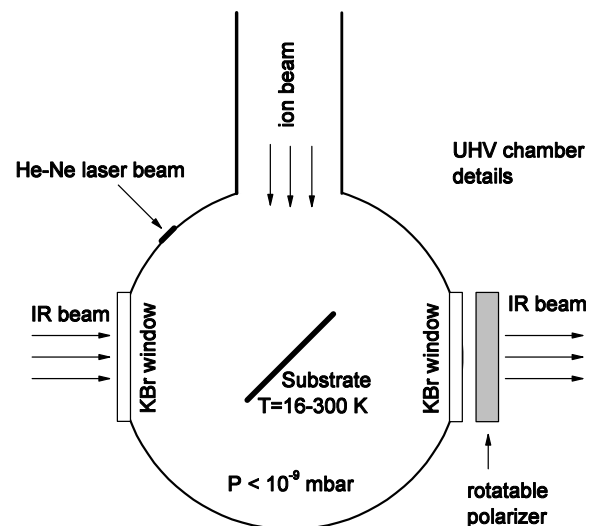


**Fig. 1.** Schematic view of the experimental set-up in the Laboratory for Experimental Astrophysics (LASp) at INAF – Osservatorio Astrofisico di Catania (Italy).

such as KBr or silicon) is placed in thermal contact with a cold finger of a closed-cycle He cryostat, whose temperature can be varied between 16 and 300 K. The substrate forms an angle of 45° both with the ion beam and with the infrared beam coming from the IR source of a spectrometer. A hole in the cold finger allows the infrared beam to be transmitted through the infrared-transparent substrate so that transmittance IR spectra can be easily taken in situ, even during ion bombardment, without tilting the sample.

A separate mixing chamber is used to prepare the gaseous mixture and to admit it into the UHV chamber by means of a needle valve. When the gaseous mixture is admitted into the main chamber, it freezes onto the substrate previously cooled forming the icy sample. During the ice growing, the thickness is monitored by checking the interference fringes produced by a He–Ne laser beam reflected at near normal incidence both by the vacuum-film and film-substrate interfaces. Laser light enters and leaves the chamber through a fused silica window whose surface is parallel to the substrate inside the chamber (see Fig. 1). Further details about the method for the thickness measurements are reported in Urso et al. (2016).

In situ infrared transmission spectra are taken at oblique incidence (45°) by a Fourier transform infrared (FTIR) spectrometer (Bruker-Vertex 70): on the wall of the UHV chamber, two KBr windows facing each other allows the infrared light coming from the spectrometer to enter and exit. On its path inside the chamber, the infrared light crosses the sample and its transparent holder. A rotatable polarizer is placed along the path of the IR beam outside the UHV chamber and allows us to take spectra both with the electric vector parallel (p-polarized) and perpendicular (s-polarized) to the plane of incidence.

The seven organic samples analysed in this work are listed in Table 1 and are produced by 200 keV proton irradiation of different frozen gases at 17 K, following a well-established laboratory procedure described hereafter. The elemental composition of the organic residues is strictly linked to the icy mixtures from which they are originated. The experimental procedure to prepare the seven organic residues is identical for all the samples in Table 1 and consists of the following six steps: (1) the chosen gaseous mixture is prepared into a mixing chamber formerly evacuated at a pressure lower than $10^{-6}$ mbar; (2) by means of

**Table 1.** The seven samples analysed in this paper.

| No. | Icy mixture (at 17 K) | Thickness ($\mu$m) | N % | C % | O % | H % | Ar % | Ion projectile | Dose (eV/16u) | Organic residue (at 290 K) |
|---|---|---|---|---|---|---|---|---|---|---|
| 1 | $N_2$:$CH_4$ (1:1) | 2.2 | 29 | 14 | – | 57 | – | 200 keV $H^+$ | 126 | Res #1 |
| 2 | $N_2$:$CH_4$:CO (1:1:1) | 1.3 | 22 | 22 | 11 | 45 | – | 200 keV $H^+$ | 106 | Res #2 |
| 3 | $N_2$:$CH_4$:$H_2O$ (1:1:1) | 1.3 | 20 | 10 | 10 | 60 | – | 200 keV $H^+$ | 122 | Res #3 |
| 4 | $N_2$:$C_8H_{18}$ (1:1) | 2.8 | 7 | 29 | – | 64 | – | 200 keV $H^+$ | 16 | Res #4 |
| 5 | $N_2$:$C_8H_{18}$ (9:1) | 2.8 | 41 | 18 | – | 41 | – | 200 keV $H^+$ | 16 | Res #5 |
| 6 | Ar:$C_8H_{18}$ (10:1) | 2.8 | – | 22 | – | 50 | 28 | 200 keV $H^+$ | 16 | Res #6 |
| 7 | CO:$CH_4$ (1:1) | 2.2 | – | 29 | 14 | 57 | – | 200 keV $H^+$ | 120 | Res #7 |

a needle valve, the prepared gaseous mixture is admitted into the main chamber where it freezes on a KBr substrate at 17 K; (3) the growth of the ice on the substrate is continuously monitored with the laser interference fringe measurement system; (4) after deposition, the infrared spectrum of the initial sample is taken; (5) then the icy mixture is bombarded by 200 keV $H^+$ ions at various irradiation steps as long as the total energy released by impinging ions reaches the required value: after each irradiation step IR spectra are taken; (6) finally, the irradiated icy mixture is gently warmed up to room temperature under vacuum condition overnight: a brownish material, the refractory organic residue, is present on the surface of the KBr substrate after all the volatile species embedded in the irradiated ice have sublimated.

For each sample discussed in this paper, we collected the IR spectra before, during and after ion irradiation, during annealing of the substrate to follow the sublimation of the volatile components and finally at room temperature. All the IR spectra shown in this paper are taken in situ, with the electric vector parallel (*p*-polarized) to the plane of incidence, resolution of $1\,cm^{-1}$ and sampling of $0.25\,cm^{-1}$. The thicknesses reported in the third column of Table 1 for each icy sample are measured before ion bombardment. Each of these frozen samples has a thickness lower than the penetration depth of the incoming ions as theoretically predicted by the SRIM code (Ziegler et al. 2008). The thicknesses of the corresponding refractory residues left over after all the volatile species in the irradiated frozen mixtures have sublimated are not directly measurable. According to the measurements presented by Baratta et al. (2015) using similar experimental conditions, we can state that the thickness of each residue typically decreases by 85–90% with respect to that of the un-irradiated ice. In this paper the energy deposited by the incoming ions to the seven samples (dose) is calculated by multiplying the ion fluence by the stopping power (i.e. the amount of energy deposited per unit path length; $eV\,cm^2\,mol^{-1}$) given by SRIM code (Ziegler et al. 2008). For each sample, the obtained value is reported in the penultimate column of Table 1: dose is given in eV/16u, which is a convenient way to characterize chemical changes and to enable a direct comparison with other experiments using various samples (Strazzulla & Johnson 1991). A more detailed description of the equipment available in the LASp can be found elsewhere (e.g. Strazzulla et al. 2001; Palumbo et al. 2004; Islam et al. 2014; Baratta et al. 2015).

### 2.2. XPS analysis

X-ray Photoelectron Spectroscopy (XPS) measurements are performed at the Dipartimento di Scienze Chimiche, Università di Catania, using a PHI ESCA/SAM 5600 Multi-technique spectrometer equipped with a Mg standard X-ray source. The pressure in the chamber is $\sim 10^{-9}$ mbar. The analyses are carried out at 45° photoelectron takeoff angle relative to the sample surface with an acceptance angle of ±7°. The binding energy (BE) scale is calibrated by centring the C1s signal of the hydrocarbon and adventitious carbon component at 285.0 eV.

Measurements of XPS are performed ex situ. Hence, organic samples are extracted from the vacuum chamber in the Laboratory for Experimental Astrophysics, stored in laboratory for a time frame of some hours and then placed into the XPS vacuum chamber.

## 3. Results

### 3.1. In situ FTIR characterization

Figure 2 shows the in situ transmission infrared spectra in optical depth scale of the seven organic residues in the spectral region $4000$–$1000\,cm^{-1}$. Each spectrum has been collected at room temperature the day after the ion irradiation of the corresponding icy mixture. In situ measurements performed in the ultra-high vacuum condition prevent any contamination of the residues.

Table 1 shows which elements are present in each icy sample and their relative abundances (i.e. number of atoms) before ion bombardment. In the following subsections, to facilitate the discussion, we have divided the IR spectra into three different spectral regions: (1) $3900$–$2300\,cm^{-1}$; (2) $2300$–$2000\,cm^{-1}$; (3) $1900$–$1000\,cm^{-1}$.

### 3.1.1. Spectral region: $3900$–$2300\,cm^{-1}$

Keeping in mind the elemental composition of the icy mixtures from which the seven organic residues are prepared, the possible functional groups falling in the spectral region $3900$–$2300\,cm^{-1}$ are: –NH– , –$NH_2$, –OH, –$CH_3$, and –$CH_2$–.

We now consider Fig. 3: Res #2 and Res #3 exhibit a broad structured band between 3500 and $2500\,cm^{-1}$ probably due to –$NH_2$ and –NH– (primary and secondary amine functional groups respectively) and –OH functional groups, with an overlapping of C–H stretching features observed on top of this broad band (Baratta et al. 2015; Materese et al. 2015). Res #1 and Res #5 display similar features due to the amines and an overlapping of C–H (Imanaka et al. 2004). In this case we can exclude the contribution of –OH functional groups because Sample #1 and Sample #5 do not contain any oxygen-bearing species; furthermore the measurements are performed in situ in the ultra-high vacuum condition and thus we can exclude any contamination into the residue.
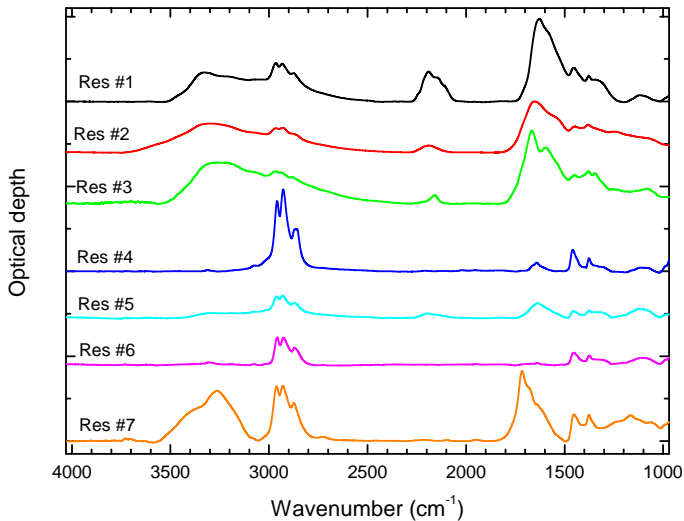
**Fig. 2.** Infrared spectra of the seven organic residues analysed in this work. Spectra are taken in situ at room temperature and are vertically shifted for clarity.



**Fig. 3.** Infrared spectra (3900–2300 cm$^{-1}$ region) of the seven organic residues analysed in this work. Spectra are collected in situ at room temperature.



**Fig. 4.** Infrared spectra (2300–2000 cm$^{-1}$ region) of the seven organic residues analysed in this work. Spectra are collected in situ at room temperature.

Looking at Fig. 3, we notice that the seven residues exhibit three features close to each other (at 2960, 2927 and 2870 cm$^{-1}$) peculiar of the aliphatic C–H bonds. In particular, the 2870 cm$^{-1}$ and 2960 cm$^{-1}$ bands are attributed respectively to –CH$_3$ symmetric and asymmetric stretching, while the 2927 cm$^{-1}$ band is attributed to –CH$_2$ symmetric stretching (Gautier et al. 2012; Greenberg et al. 1995). We can also note that the intensity of these three features varies according to the residue taken into consideration, mostly depending on the elemental abundances of the icy mixture before ion irradiation. For instance, Sample #4 and Sample #5 are both composed of nitrogen (N$_2$) and octane (C$_8$H$_{18}$) but with different initial ratio (see Table 1): in Sample #4 N/C is 0.25 while in Sample #5 N/C is greater than two. As Sample #4 and Sample #5 had identical thickness and suffered the same dose, we can directly compare the IR spectra of the two corresponding residues (namely Res #4 and Res #5): the lower availability of nitrogen in Sample #4 promotes the formation of the aliphatic chains and inhibits the formation of nitriles. Hence, Res #4 exhibits CH stretching mode features more intense and CN features less intense than those observed in Res #5 (see more details in Sect. 3.1.2). The organic residue Res #7, originated by ion irradiation of the icy mixture containing carbon monoxide (CO) and methane (CH$_4$), exhibits a multi-component band between 3600 and 3060 cm$^{-1}$ mainly due to O–H bonds.

### 3.1.2. Spectral region: 2300–2000 cm$^{-1}$

As discussed elsewhere (e.g. Palumbo et al. 2000a,b), the spectral region 2300–2000 cm$^{-1}$ draws special interest from astrobiologists because the triple CN bonds of nitriles that are considered relevant to pre-biotic chemistry, fall in this region. Looking at Fig. 4, we noticed that the residues originated by icy mixtures free of nitrogen (Res #6 and Res #7) exhibit no important features in this spectral region. The IR spectrum of Res #4 shows very weak features in this spectral region: although the icy Sample #4 before ion bombardment contains nitrogen, the great availability of carbon (N/C = 0.25) promotes the formation of C–H aliphatic bonds to the detriment of CN bonds.

Vice versa, Res #1, Res #2, Res #3 and Res #5 exhibit a multi-picked band centred at about 2200 cm$^{-1}$. The vertical
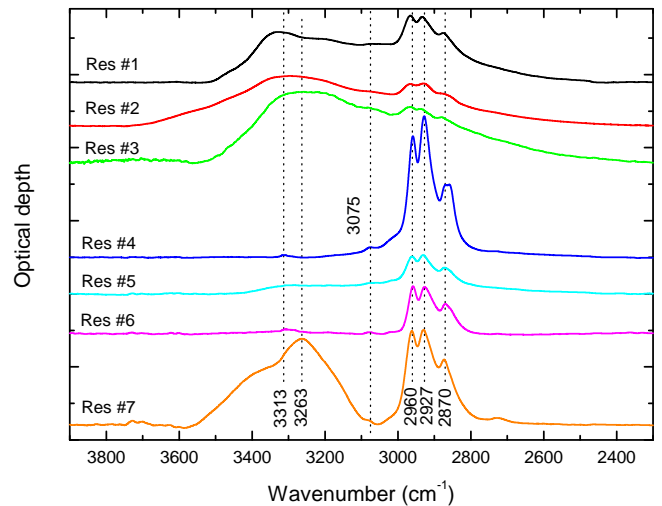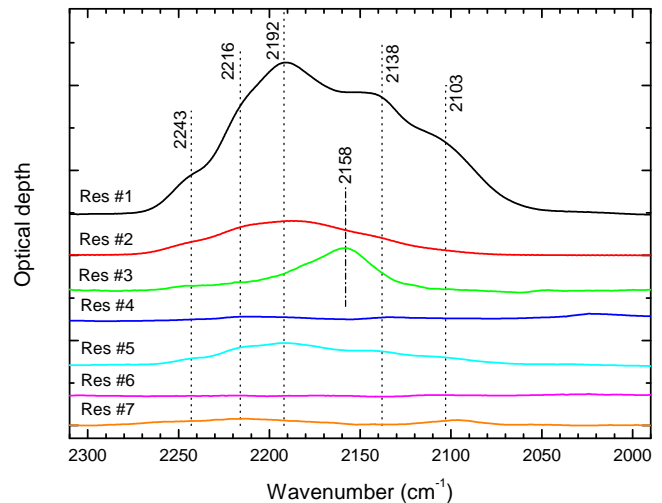
dotted lines in Fig. 4 stress five components clearly recognizable at least for Res #1 Res #2 and Res #5: two of these components (2243 and 2216 cm$^{-1}$) are commonly assigned to nitriles (–C≡N) while the remaining three (2192, 2138 and 2103 cm$^{-1}$) to isonitriles (–N≡C) (Mutsukura & Akita 1999; Imanaka et al. 2004).

The dot-dash vertical line in Fig. 4 highlights that Res #3 displays a band whose main feature is peaked at 2158 cm$^{-1}$, namely a different frequency with respect to those observed for Res #1, Res #2 and Res #5. Moreover, this band does not display the same components observed for the other residues. We can suppose that the presence of H$_2$O as component of the icy mixture (Sample #3) could affect the chemical rearrangements into the ice during both ion irradiation at 17 K and the subsequent annealing to room temperature. In order to investigate the nature of the features detected in residues Res #1, Res #2, Res #3, and Res #5 at room temperature ($T$ = 290 K), it is useful to pay attention to the evolution of the IR features in the same spectral region starting from the spectra of the corresponding icy mixtures just after ion irradiation at 17 K, during the following warm-up (e.g.
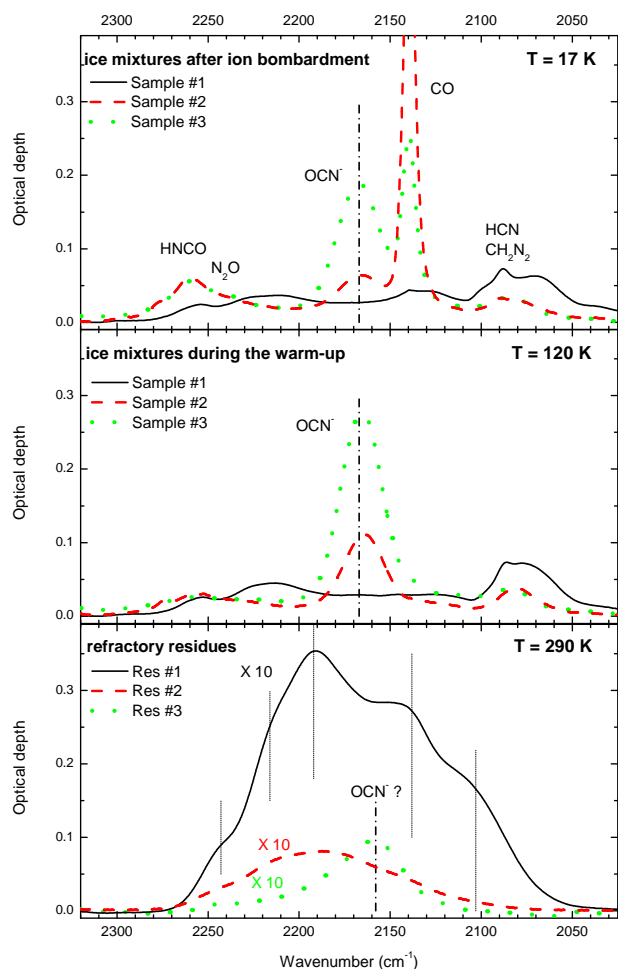
**Fig. 5.** Spectra in the 2320–2025 cm$^{-1}$ region, evolving with the temperature for three icy mixtures after ion exposure. Sample #1 (N$_2$:CH$_4$ + 200 keV H$^+$), Sample #2 (N$_2$:CH$_4$:CO + 200 keV H$^+$), and Sample #3 (N$_2$:CH$_4$:H$_2$O + 200 keV H$^+$). *Top panel*: IR spectra of the three samples at 17 K, just after ion irradiation. Central panel shows the IR spectra of the three samples at 120 K, during warm-up. *Bottom panel*: IR spectra of the three corresponding refractory organic residues at room temperature, magnified 10 times for the sake of clarity.



**Fig. 6.** Evolution of the position of the band assigned to OCN$^-$ during the slow warm-up of the irradiated Sample #3 from 17 K to room temperature.

oxygen-bearing species (such as OCN$^-$) do not contribute to the 2200 cm$^{-1}$ band observed in the organic residues at room temperature.

As highlighted in the bottom panel of Fig. 5, the IR spectrum of Res #3 at room temperature exhibits a band peaked at 2158 cm$^{-1}$, whose attribution is not clear. The position could suggest that the band may be due to OCN$^-$ trapped in the organic residue at room temperature. In fact starting from the position of the OCN$^-$ band in the irradiated Sample #3 at 17 K (2167 cm$^{-1}$), we monitored the peak position of this band at different temperatures during the whole warm-up of the icy sample and we recorded a gradual shift towards lower wavenumbers as the sample temperature increases, reaching 2160 cm$^{-1}$ at 260 K (see Fig. 6). Then the frequency of the peak recorded for the refractory residue at room temperature (2158 cm$^{-1}$) could be compatible with the trend of the recorded peak position of the OCN$^-$ ion into the ice.

Our experimental results show that the organic residues containing nitrogen, carbon and hydrogen present similar features in the spectral region 2300–2000 cm$^{-1}$. That is clear looking at Fig. 7, where the spectra of Res #4 and Res #5 are magnified six and three times respectively to facilitate the comparison with the spectrum of the residue Res #1. In particular, both Res #1 and Res #5 exhibit the five features stressed by the vertical lines in Fig. 7 and already mentioned. Moreover the two overall structured bands look very similar one another, although Sample #1 and Sample #5 had different composition and N to C ratio before ion bombardment and they suffered different amount of energy deposited by incoming ions. Even Res #4 presents the same five components although with slight differences: in fact the overall profile of the band is different and the features at 2192, 2138 and 2103 cm$^{-1}$ present slight shifts towards lower wavenumbers. Since Res #4 and Res #5 come from two icy mixtures with identical molecular composition (albeit with different ratio) and suffer identical dose, the differences observed in the two spectra are certainly attributable to the different values of atomic N/C.

### 3.1.3. Spectral region: 1900–1000 cm$^{-1}$

The specific assignment of the features in the spectral region 1900–1000 cm$^{-1}$ is not easy because different functional groups fall in this region often overlapping one another. Looking at Fig. 8, we observe an overlap of features in the spectra of the

at 120 K) and finally at room temperature. To do that, we consider an icy mixture containing N, C, and H (Sample #1), and two different icy mixtures containing N, C, H, and O (Sample #2 and Sample #3). Top panel of Fig. 5 shows the IR spectra of the icy samples #1, #2, and #3 at the end of the ion bombardment at 17 K: Sample #2 and Sample #3 exhibit a feature peaked at 2167 cm$^{-1}$. The nature of this band, also detected in some astrophysical sources at low temperature (e.g. Pendleton et al. 1999; Pontoppidan et al. 2003; van Broekhuizen et al. 2005), has been largely discussed in the past. Now it is commonly attributed to the OCN$^-$ ion (Hudson et al. 2001; Novozamsky et al. 2001; Bennett et al. 2010). As shown in the central panel of Fig. 5, the OCN$^-$ band observed in the two samples is still detected at 120 K during the warm-up, with a greater strength and a slightly different peak position. The absence of this band both at 17 K and at 120 K in the spectrum of Sample #1 is due to the lack of oxygen-bearing species in the initial icy mixture. Nevertheless, at room temperature, the refractory residues Res #1 and Res #2 display a 2200 cm$^{-1}$ multi-peaked band having shape and features very similar to each other (see the bottom panel of Fig. 5) and thus due to the same functional groups. This indicates that
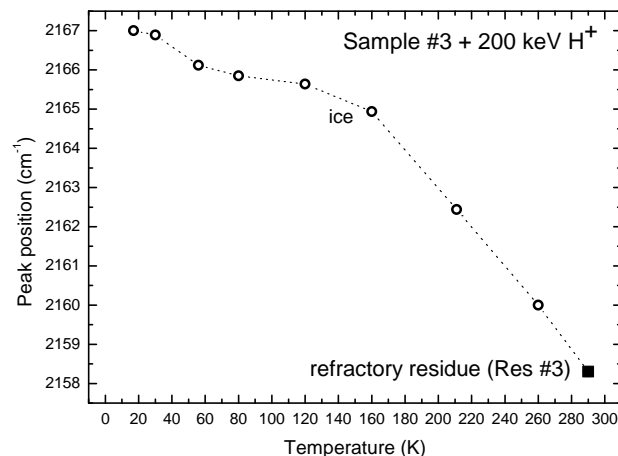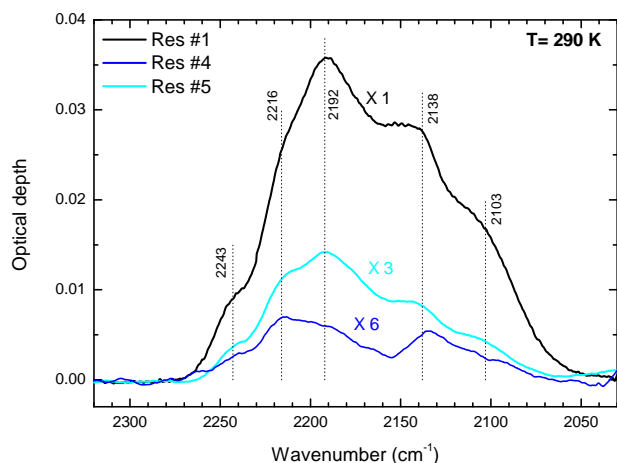
**Fig. 7.** Infrared spectra (2300–2000 cm$^{-1}$ region) of Res#1, Res #4 and Res #5. The spectra of Res #4 and Res #5 are magnified six and three times respectively for the sake of clarity.
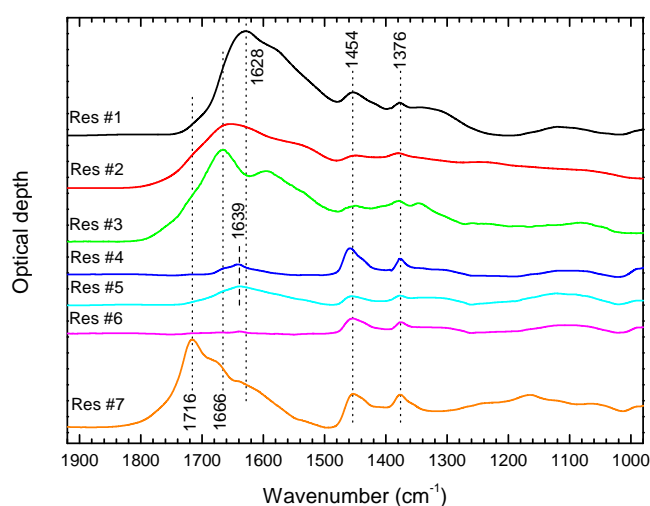


**Fig. 8.** Infrared spectra (1900–1000 cm$^{-1}$ region) of the seven organic residues analysed in this work. Spectra are collected in situ at room temperature.

**Table 2.** Elemental composition of three organic residues by XPS analysis.

| Res #1 | Peak position (eV) | | | |
|---|---|---|---|---|
| C (73.4%) | 285.0 | 286.5 | 288.1 | – |
| N (21.8%) | 399.6 | – | – | – |
| O (3.6%) | 532.2 | – | – | – |
| Res #4 | Peak position (eV) | | | |
| C (94.0%) | 285.0 | 286.5 | 288.1 | – |
| N (2.4%) | 399.7 | – | – | – |
| O (3.6%) | 532.6 | – | – | – |
| Res #3 | Peak position (eV) | | | |
| C (64.5%) | 285.0 | 286.5 | 288.1 | 289.0 |
| N (18.4%) | 400.1 | 398.5 | – | – |
| O (17.1%) | 532.6 | 531.5 | – | – |

1740 and 1480 cm$^{-1}$ exhibits at least two peaks at about 1630 and 1580 cm$^{-1}$ due to different functional groups such as C=N heteroaromatics, C=C aromatics (stretching) and –NH$_2$ (bending). Res #4, Res #5, and Res #6 do not contain oxygen and their spectra do not display intense features in this region: the weak feature at 1639 cm$^{-1}$ observed in the spectrum of Res #4 and Res #5 (see vertical line in Fig. 8) may be due to regular imines (CN double bonds).

### 3.2. XPS spectroscopy

X-ray photoelectron spectroscopy analyses are performed on three organic residues (Res #1, Res #3, and Res #4) with the aim of evaluating the surface elemental composition and the main organic chemical functional groups present in the samples, keeping in mind the elements of the respective icy mixtures. The observed atomic concentrations (%) are reported in Table 2.

The XPS spectrum of the residue Res #1 reveals the presence of carbon (~73.4%), nitrogen (~21.8%) and a small amount of oxygen (less than 4%). In the high-resolution spectrum of the C1s region (Fig. 9), we can observe the presence of a main band centred at 285.0 eV (blue line), a shoulder positioned at binding energy of 286.5 eV (red line) and a very weak band detected at 288.1 eV (green line). The band at 285.0 eV is compatible with the presence of the CH$_x$, C–C or C=C moieties, which is consistent with the detection of the alkyl and unsaturated groups in the FTIR spectra (e.g. the features due to the C–H stretching modes in Fig. 2). The C1s component located at 286.5 eV can be described as the contribution from carbon and nitrogen species (C–N, C=N and C≡N) as discussed by Nuevo et al. (2011). The low-intensity band positioned at the highest binding energy, specifically at 288.1 eV, is likely due to bonds formed between carbon and oxygen, such as carbonyl groups (e.g. Kaba et al. 2005; Ahmed et al. 2013). The presence of oxygen in Res #1 is not expected because of the lack of oxygen-bearing species in the icy mixture of Sample #1; nonetheless, the formation of C=O species can reasonably occur as the result of the reaction of the surface reactive species with the atmospheric H$_2$O and/or O$_2$. The N1s XPS region of Res #1 shows a band positioned at 399.6 eV with a FWHM of 2.4 eV (Fig. 9). The large width of the band suggests the presence of a variety of nitrogen-containing species. Additionally, the BE is lower than the typical BE value found for single N–H, N–C bonds (~400.0 eV), suggesting that species with electron-rich nitrogen functionalities (e.g. C=N/C≡N) are present (e.g. Hsu et al. 2010; Matsuoka et al. 2012). This is strongly supported by the

seven residues due to a blend of the features of different functional groups. According to the assignment reported in literature (e.g. Imanaka et al. 2004; Dartois et al. 2013; Materese et al. 2015), carbonyl stretching modes (C=O) fall at about 1700 cm$^{-1}$, sp$^2$ C=C and C=N stretching modes fall between 1650 and 1500 cm$^{-1}$ and NH$_2$ bending modes at about 1600 cm$^{-1}$. The presence or the intensity of these features depends on the relative abundances of the elements N, C, O, and H in the initial icy mixtures.

All the seven residues display two features at 1454 and 1376 cm$^{-1}$ that we can assign to the aliphatic C–H bending modes (Quirico et al. 2008). The presence of these two bands is consistent with the detection of the three bands due to C–H stretching bonds and falling respectively at 2960, 2927 and 2870 cm$^{-1}$ (Fig. 3).

Res #7 contains C, O, and H elements and its spectrum displays a sharp band peaked at 1716 cm$^{-1}$ due to C=O stretching mode probably indicating the presence of aldehydes, ketones and/or carboxylic acids. The 1716 cm$^{-1}$ feature could also be present in the spectra of Res #2 and Res #3 blended in the broad band centred at about 1600 cm$^{-1}$. Res #1 contains N, C, and H elements and its multi-component broad band between
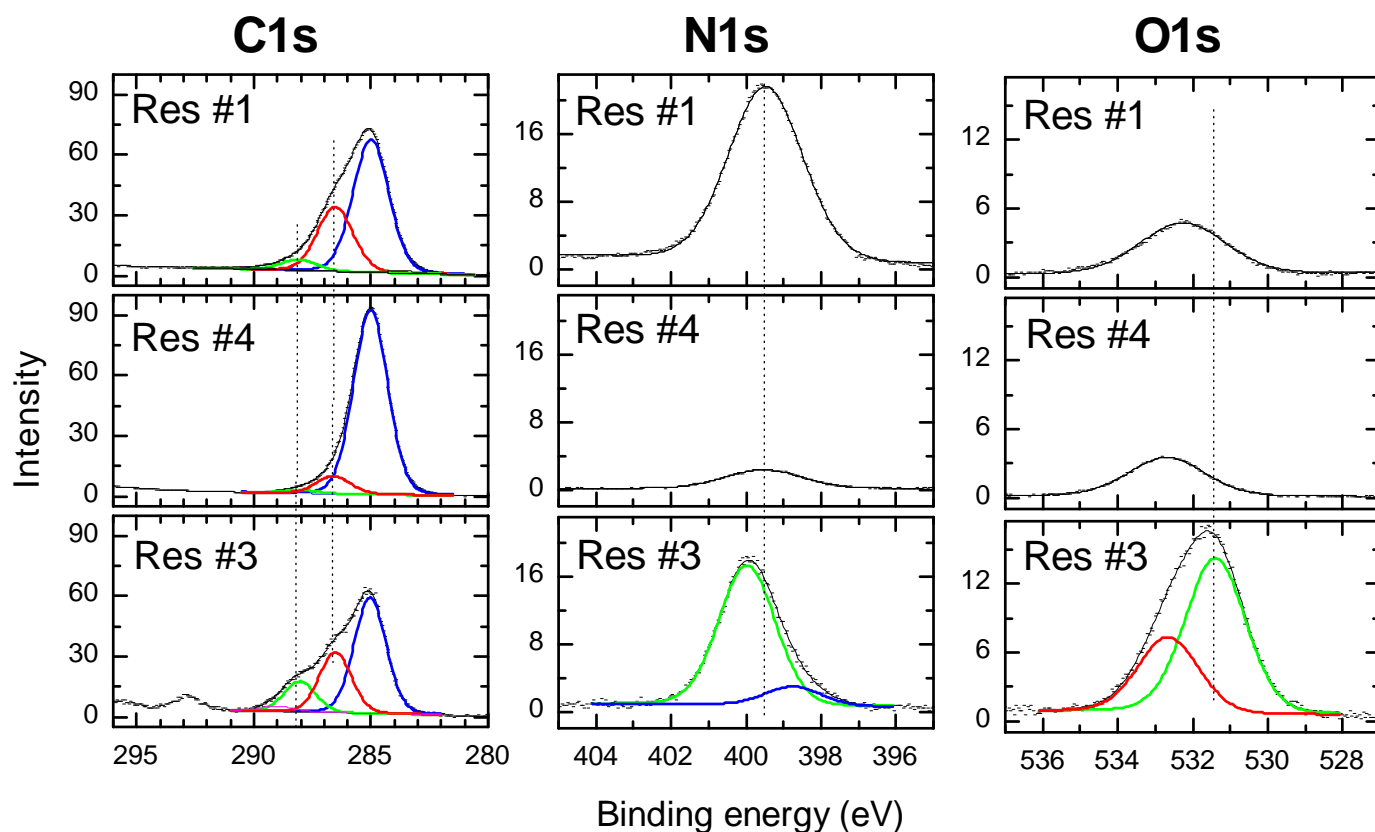
## C1s  N1s  O1s



**Fig. 9.** XPS spectra of Res #1, Res #3, and Res #4 in the C1s, N1s, and O1s spectral regions.

FTIR features showing the presence of imine ($\sim$1640 cm$^{-1}$) and nitrile groups ($\sim$2200 cm$^{-1}$), as well of amines ($\sim$3400 cm$^{-1}$). It is to be noticed, in addition, that there is a good correspondence between the XPS percentage of the band at 286.5 eV in the C1s region (22.5%) and the atomic percentage of the nitrogen in the sample (21.8%, see Table 2). The weak signal in the O1s region (Fig. 9) consists of a broad band (FWHM = 2.6 eV) with the maximum positioned at 532.2 eV, which is compatible with the presence of different typologies of C=O bonds. The presence of the oxygen-containing moieties in the sample is negligible and essentially due to the surface or environment interaction.

The XPS analysis of Res #4, obtained by ion irradiation of the icy mixture $N_2$:$C_8H_{18}$ (1:1), indicates the presence of carbon (94.0%), nitrogen (2.4%) and, similarly to the Res #1, a small amount of oxygen (3.6%). If compared to Res #1, the amount of nitrogen is notably reduced by a factor of ten. As results, Res #4 is mainly constituted of C–C/C=O and C–H containing species. The different compositions observed in the two samples Res #1 and Res #4 are roughly ascribable to the following factors: i) the different C to N atomic ratio of the two mixtures; and ii) the different reactivity of the two hydrocarbons. Although different concentrations are observed, similar organic functionalities are found in both residues. The C1s spectral region of the Res #4 (Fig. 9) shows the predominant presence of the C1s component centred at 285.0 eV due to the $CH_x$, C–C and C=C moieties, a small band at 286.5 eV and a negligible band at 288.1 eV. The predominant presence of $CH_x$, C–C and C=C moieties is also supported by FTIR data which show intense modes of the aliphatic $CH_x$ at 2900 cm$^{-1}$. The component at 286.5 eV is attributed to the presence of the CN species similarly to the N1s XPS spectrum of the Res #1. In this case,

the contribution at higher BE values (288.1 eV) associated to the presence of oxidized carbon species is negligible. Despite the lower intensity, the shape and the position of N1s band of the Res #4 (Fig. 9) are similar to those observed for Res #1 (FWHM = 2.4 eV and BE = 399.7 eV), indicating the presence of C=N/C≡N. The small amount of nitrogen detected by XPS is in agreement with the low intensity of the FTIR modes at 2200 cm$^{-1}$ and at 1640 cm$^{-1}$ associated to –C≡N/–N≡C and C=N respectively. Finally, the low O1s band (Fig. 9) suggests the presence of oxidized species, due to the interaction of the surface with the environment analogously with Res #1. Therefore the XPS characterization of Res #1 and Res #4 indicates that either methane or octane in presence of $N_2$ in the irradiated icy mixtures leads to the formation of C–C, C=C, and C–N, C=N, and C≡N functionalities. However, different percentages are found due to different lengths of the hydrocarbon chains.

In order to better elucidate the effect of the presence of water in the icy mixture, we analysed Res #3, the organic residue produced from the proton bombardment of the icy mixture $N_2$:$CH_4$:$H_2O$ (1:1:1). The X-ray photoelectron spectroscopy analysis shows the presence of carbon ($\sim$64.5%), nitrogen ($\sim$18.4%) and oxygen ($\sim$17.1%). In this case, the fraction of oxygen is greater compared to Res #1 and Res #4 because of the presence of water in the frozen gas mixture before ion irradiation. The high-resolution spectrum of the C1s region (Fig. 9) shows a structured signal that can be fitted with three main components picked at 285.0, 286.5, 288.1 and a small contribution at 289.0 eV. The latter, which is assigned to the presence of carboxylic acid (–COOH), is not revealed in the spectra of the other two samples Res #1 and Res #4 and it is reasonably due to the action of the water in the icy mixture. The contribution relative to the hydrocarbon species lying at 285.0 eV is lower

compared to the contribution of these species observed in the previous residues in agreement with the lower intensity of the $CH_x$ features (at about 2900 cm$^{-1}$) observed in the FTIR spectra. The band at 286.5 eV is associated to the contributions from CN (C–N, C=N, C≡N) groups similarly to the previous residues. In this case some contribution due to C–O containing species cannot be excluded. It is of interest to notice that the band at 288.1 eV, also present in the XPS spectra of Res #1 and Res #4 as result of C-oxidation due to oxygen contamination, is significantly increased in the spectrum of the Res #3, as expected for the presence of the water in the mixture. We note that in the literature, the position of this band could be associated to the C of N=C=O$^-$ ions (Mavis & Akinc 2006). However the presence of amides (>N–C=O) cannot be excluded. The formation of OCN$^-$ or amides could be due to the interaction between water and the organic C≡N residues (e.g. hydrolysis). In order to better clarify this point, it is important to compare the N1s and O1s spectral features of the samples obtained in presence (Res #3) and in absence of water (Res #1 and Res #4). The N1s signal of Res #3 appears asymmetric and narrower with respect to the two previous cases, showing a main band positioned at 400.1 and a much smaller contribution at 398.5 eV both with FWHM of 1.8 eV. The interpretation of the peak at 400.1 eV is not unambiguous, being compatible with the presence of amine and amides (e.g. Amaral et al. 2005; Ramanathan et al. 2005; Rao et al. 2014). The band at 398.5 eV can be due to the presence of electron-rich nitrogen atoms as in the case of aromatic imine (e.g. Yamashige et al. 2005; Kretschmann et al. 2007). We note the lack of the component lying around 399.6–399.7 eV, associated to the nitrile groups (Gammon et al. 2003). This could be related to the abrupt decrease of the intensity of the IR band peaked at 2158 cm$^{-1}$ over time: in fact, following by IR spectroscopy the natural evolution over time of a organic residue identical to Res #3, we note that the band peaked at 2158 cm$^{-1}$ exhibits a gradual reduction in intensity over time, decreasing by 60% after two weeks and almost by 100% after 150 days. In addition, the O1s spectrum of Res #3 presents an asymmetric signal with a main component at 531.5 eV and a shoulder at 532.6 eV. The latter is commonly attributed to generic C–O/C=O bonds, whilst the band at a value as low as 531.5 eV is typically reported for oxygen with a partial negative character as expected for OCN$^-$ or amides (e.g. Clochard et al. 2007; Rück-Braun et al. 2013). Thus XPS data support the spectral findings obtained by the FTIR technique, which show notable differences in the absorption features between 1600–1700 cm$^{-1}$. Our results indicate that the composition of the organic residue is strongly affected by the presence (or the lack) of H$_2$O which induces the formation of OCN$^-$ functionalities.

## 4. Discussion

The comparative study of the seven organic residues presented in this work points out the chemical similarities and differences between them. For instance, all the solid samples here analysed display the aliphatic C–H stretching (2960, 2927 and 2870 cm$^{-1}$) and bending (1454 and 1376 cm$^{-1}$) features, namely every icy mixture containing hydrocarbons, if subjected to ion irradiation, produces organic residues having long aliphatic chains. The intensity of these features depends on the relative atomic abundance and on the total amount of energy released by ions on the ice.

If the icy mixture contains nitrogen, as well as hydrogen and carbon (e.g. Sample #1, Sample #4, and Sample #5), the proton bombardment and the following annealing to room temperature

produces an organic residue whose infrared spectrum exhibits a structured feature in the region 2300–2000 cm$^{-1}$ due to nitrile and isonitrile terminal groups. Indeed, we can assert that the three residues, Res #1, Res #4, and Res #5, contain similar functional groups as the same five components of the 2200 cm$^{-1}$ feature are recognizable for each sample (see Fig. 7). In this paper, Res #1 is taken as example of organic residue obtained after ion irradiation of an icy mixture containing carbon, hydrogen and nitrogen, but free of oxygen. Looking at the spectrum of Sample #1 just after proton bombardment at 17 K and at 120 K during the warm-up, the features observed in the region 2300–2000 cm$^{-1}$ are weaker than those observed for Sample #2 and Sample #3 (see top and central panel of Fig. 5). However, at room temperature, Res #1 displays a strong and structured feature in the same spectral region. This demonstrates that additional chemical changes occur at temperatures higher than 120 K during the warm-up, when molecules and radicals become more mobile and could react each other more readily.

Both Sample #2 and Sample #3 contain hydrogen, carbon, nitrogen, and oxygen. However, their corresponding organic residues (Res #2 and Res #3) do not display the same functional groups that give rise to the 2200 cm$^{-1}$ feature. This is evident looking at the infrared spectra of the two samples in the region 2300–2000 cm$^{-1}$: both show two multi-peaked bands, but with profiles and components different one another. Thus Res #2 exhibits a 2200 cm$^{-1}$ feature comparable to those observed for Res #1, Res #4, and Res #5 (see the bottom panel of Fig. 5), whereas Res #3 displays a quite sharp feature centred at 2158 cm$^{-1}$. We think that the presence of water as component of Sample #3 can affect the chemical rearrangements during proton bombardment at 17 K and especially during the annealing to room temperature, preventing or reducing the formation of molecules containing nitrile and iso-nitrile groups and encouraging the formation of molecules containing amide groups, as already stressed by commenting the XPS spectra in the previous section. Looking at the IR spectrum of Res #3, we are not sure about the chemical groups responsible of the band centred at 2158 cm$^{-1}$, even if we hypothesize a contribution of OCN$^-$ still trapped in the organic residue (Res #3) at room temperature. OCN$^-$ ion is one of the new species formed at 17 K after energetic processing of a frozen icy mixture containing oxygen, carbon and nitrogen bearing species (e.g. van Broekhuizen et al. 2005). Indeed it has been detected both in Sample #2 and in Sample #3 after proton bombardment (see the top panel of Fig. 5). During the annealing of Sample #3, we have recorded the OCN$^-$ peak position as a function of the sample temperature: we recognize a gradual shift towards lower wavenumbers as the sample temperature increases, from 2167 cm$^{-1}$ at 17 K– 2160 cm$^{-1}$ at 260 K. Therefore the frequency of the peak observed for the refractory residue at room temperature (2158 cm$^{-1}$) could be compatible with the trend of the recorded peak position of the OCN$^-$ ion into the ice, as shown in Fig. 6.

In this section, we are mainly focusing on the spectral region 2300 – 2000 cm$^{-1}$ due to its link with astrobiological studies. In fact the triple CN bond stretching mode of nitriles considered relevant to pre-biotic chemistry falls in this region. The role of nitriles in formation of various pre-biotic compounds has been illustrated by Matthews & Minard (2006). Our experimental results demonstrate that the presence of oxygen in the icy samples is not necessary for the formation, at room temperature, of the multi-component band at 2200 cm$^{-1}$ that we identify with nitrile (–C≡N) and isonitrile (–N≡C) functional groups.

The refractory residues containing nitrogen, such as those analysed in this paper, seem to be good analogues of the

materials formed in the outermost solar system, in particular on the surface of those objects whose temperature allow the condensation of nitrogen. For instance, some ultra carbonaceous Antarctic micro-meteorites exhibit IR signatures that are similar to those observed in the organic residues analysed in this work (Dartois et al. 2013, 2018). In particular some of these micro-meteorites present the 2200 cm$^{-1}$ –C≡N nitrile feature. It is thought that this high organic carbon content (>50% vol.) and high N/C (e.g. 0.12 in DC65) micro-meteorites originated in the outer solar system beyond the nitrogen snow-line, for example in an Oort-cloud comet in billions of years by cosmic ray irradiation (Dartois et al. 2013, 2018).

## 5. Conclusion

The experimental results presented so far point out that ion irradiation of simple ice mixtures containing C, N, O, and H atoms, leads to the formation of organic residues that are stable at room temperature. Infrared and XPS spectroscopies have shown that the organic residues exhibit a high chemical complexity pointed out by the presence of different functional groups such as amines, amides and nitriles. Further analysis using other techniques (such as gas chromatography and mass spectroscopy) would give additional information on the complex organic content of the solid samples discussed in this paper.

Material similar to that synthesized in laboratory could have been produced on the surfaces of solar system objects beyond the nitrogen snow-line, such as comets in the Oort cloud, by galactic cosmic-ray irradiation. When a comet enters in the inner solar system and the coma develops, a large quantity of dust is lost. This dust constitutes a significant fraction of the IDPs that reach the Earth atmosphere. Hence organic material analogue to that we synthesized in laboratory could have reached the early Earth. One of the key points for the synthesis of the first biomonomers, is the availability of suitable precursor organics in primitive Earth conditions (Ruiz-Mirazo et al. 2014). It has been estimated that the delivery of organic carbon (mostly by IDPs, comets and meteorites) on the early Earth was of the order of $10^8$ kg yr$^{-1}$, or $10^{16}$ kg per 100 million years (Chyba & Sagan 1992). Since there is about $6 \times 10^{14}$ kg of organic matter in the present biosphere, it is likely that the role of extraterrestrial organics was significant (Ruiz-Mirazo et al. 2014). Among the organics that could have had a role in providing the bricks from which life could be initiated, there are the nitriles. Indeed nitriles could be key intermediates in forming amino acids thus providing one of the basic ingredients for life (e.g. Kaiser & Balucani 2001; Matthews & Minard 2006).

## References

Ahmed, M. H., Byrne, J. A., McLaughlin, J., & Ahmed, W. 2013, JBN, 4, 194
Altwegg, K., Balsiger, H., Bar-Nun, A., et al. 2016, Sci. Adv., 2, 5
Amaral, I. F., Granja, P. L., & Barbosa, M. A. 2005, J. Biomater Sci. Polym. Ed., 16, 1575
Baratta, G. A., Chaput, D., Cottin, H., et al. 2015, Planet Space Sci., 118, 211
Bennett, C. J., Jones, B., Knox, E., et al. 2010, ApJ, 723, 641
Brunetto, R., Barucci, M. A., Dotto, E., & Strazzulla, G. 2006, ApJ, 644, 646
Chyba, C., & Sagan, C. 1992, Nature, 355, 125
Clochard, M., Cuscito, O., Berthelot, T., et al. 2007, React (Polym: Funct). 77
Cobb, A. K., Pudritz, R. E., & Pearce, B. K. D. 2015, ApJ, 809, 6
Dartois, E., Engrand, C., Brunetto, R., et al. 2013, Icarus, 224, 243
Dartois, E., Engrand, C., Duprat, J., et al. 2018, A&A, 609, A65
d'Hendecourt, L. B., Allamandola, L. J., Grim, R. J. A., & Greenberg, J. M. 1986, A&A, 158, 119
Fedo, C. M., Whitehouse, M. J., Kamber, B.S., et al. 2006, Phil. Trans. R. Soc. London Ser. B, 361, 851
Fedoseev, G., Ioppolo, S., Zhao, D., Lamberts, T., & Linnartzet, H. 2015, MNRAS, 446, 439
Ferini, G., Baratta, G. A., & Palumbo, M. E. 2004, A&A, 414, 757
Gammon, W. J., Kraft, O., Reilly, A. C., & Holloway, B. C. 2003, Carbon, 41, 1917
Gautier, T., Carrasco, N., Mahjoub, A., et al. 2012, Icarus, 221, 320
Greenberg, J. M., Yencha, A. J., Corbett, J. W., & Frisch, H. L. 1972, Mem. Soc. R. Sci. Liege, 425, 6$^e$ serie, tome III
Greenberg, J. M., Li, A., Mendoza-Gómez, C. X., et al. 1995, ApJ, 455, L177
Hsu, C. H., Wu, H. M., & Kuo, P. L. 2010, Chem. Commun., 46, 7628
Hudson, R. L., Moore, M. H., & Gerakines, P. A. 2001, ApJ, 550, 1140
Hudson, R. L., Moore, M. H., Dworkin, J. P., Martin, M. P., & Pozun, Z. D. 2008, Astrobiology, 8, 771
Imanaka, H., Khare, B. N., Elsila, J. E., et al. 2004, Icarus, 168, 344
Islam, F., Baratta, G. A., & Palumbo, M. E. 2014, A&A, 561, A73
Kaba, M., Raklaoui, N., Guimon, M. F., & Mas, A. 2005, J. Appl. Polym. Sci., 97, 2088
Kaiser, R. I., & Balucani, N. 2001, Acc. Chem. Res., 34, 699
Kretschmann, A., Walz, M. M., Flechtner, K., Steinrücka, H. P., & Gottfried, J. M. 2007, Chem. Commun., 568,
Materese, C. K., Cruikshank, D. P., Sandford, S. A., et al. 2014, ApJ, 788, 111
Materese, C. K., Cruikshank, D. P., Sandford, S. A., Imanaka, H., & Nuevo, M. 2015, ApJ, 812, 150
Matsuoka, M., Isotani, S., Mansano, R. D., et al. 2012, WJNSE, 2012, 92
Matthews, C. N., & Minard, R. D. 2006, FaDi, 133, 393
Mavis, B., & Akinc, M. 2006, Chem. Mater., 18, 5317
Moore, M. H., Hudson, R. L., & Gerakines, P. A. 2001, Spectrochim. Acta A, 57, 843
Muñoz Caro, G. M., Meierhenrich, U. J., Schutte, W. A., et al. 2002, Nature, 416, 403
Muñoz Caro, G. M., Dartois, E., Boduch, P., et al. 2014, A&A, 566, A93
Mutsukura, N., & Akita, K. 1999, Thin Solid Films, 349, 115
Novozamsky, J. H., Schutte, W. A., & Keane, J. V. 2001, A&A, 379, 588
Nuevo, M., Bredehöft, J. H., Meierhenrich, U. J., d'Hendecourt, L., & Thiemann, W. H. P. 2010, AsBio, 10, 245
Nuevo, M., Milam, S. N., Sandford, S. A., et al. 2011, AdSpR, 48, 1126
Öberg, K. I., Garrod, R. T., van Dishoeck, E. F., & Linnartz, H. 2009, A&A, 504, 891
Palumbo, M. E., Strazzulla, G., Pendleton, Y. J., & Tielens, A. G. G. M. 2000a, ApJ, 534, 801
Palumbo, M. E., Pendleton, Y. J., & Strazzulla, G. 2000b, ApJ, 542, 890
Palumbo, M. E., Ferini, G., & Baratta, G. A. 2004, AdSpR, 33, 49
Pendleton, Y. J., Tielens, A. G. G. M., Tokunaga, A. T., & Bernstein, M. P. 1999, ApJ, 513, 294
Pontoppidan, K. M., Fraser, H. J., Dartois, E., et al. 2003, A&A, 408, 981
Quirico, E., Montagnac, G., Lees, V., et al. 2008, Icarus, 198, 218
Ramanathan, T., Fisher, F. T., Ruoff, R. S., & Brinson, L. C. 2005, Chem. Mater., 17, 1290
Rao, K. S., Senthilnathan, J., Ting, J. M., & Yoshimura, M. 2014, Nanoscale, 2014, 12758
Rothard, H., Domaracka, A., Boduch, P., et al. 2017, J. Phys. B At., Mol. Opt. Phys., 50, 062011
Ruiz-Mirazo, K., Briones, C., & de la Escosura, A. 2014, Chem. Rev., 114, 285
Rück-Braun, K., Petersen, M. A., Michalik, F., et al. 2013, Langmuir, 29, 11758
Strazzulla, G., Baratta, G. A., & Palumbo, M. E. 2001, Spectrochim. Acta A, 57, 825
Strazzulla, G., & Johnson, R. E. 1991, Comets in the post-Halley Era, 1, ASSL Series, Dordrecht, 243
Urso, R. G., Scirè, C., Baratta, G. A., Compagnini, G., & Palumbo, M. E. 2016, A&A, 594, A80
Urso, R. G., Scirè, C., Baratta, G. A., et al. 2017, PCCP, 19, 32
van Broekhuizen, F. A., Pontoppidan, K. M., Fraser, H. J., & van Dishoeck, E. F. 2005, A&A, 441, 249
Yamashige, H., Matsuo, S., Kurisaki, T., & Wakita, H. 2005, Anal. Sci., 21, 634
Ziegler, J. F., Biersack, J. P., & Ziegler, M. D. 2008, The Stopping and Range of Ions in Solids (New York: Pergamon Press), 321